HIGHLY EFFCIENT QUASI-OPTICAL MODE CONVERTER SYSTEM FOR A 1 MW, 140 GHZ, CW GYROTRON

M. Thumm [1, 2], A. Arnold [1, 2], G. Dammertz[1], G. Michel [3], J. Pretterebner [4], D. Wagner [5], X. Yang [1]

[1]Forschungszentrum Karlsruhe, Association EURATOM-FZK, IHM, 76021 Karlsruhe, Germany
[2] Universitaet Karlsruhe, IHE, 76128 Karlsruhe, Germany
[3]Max-Planck-Institut fuer Plasmaphysik, Association EURATOM-IPP, 17491 Greifswald, Germany
[4]DaimlerChrysler AG, 70546 Stuttgart, Germany
[5] Max-Planck-Institut fuer Plasmaphysik, Association EURATOM-IPP, 85748 Garching, Germany

e-mail: manfred.thumm@ihm.fzk.de

A highly efficient quasi-optical mode converter system with several novel features has been designed and tested at Forschungszentrum Karlsruhe (FZK). The mode converter employs a dimpled-wall waveguide section and a helical-cut launching aperture as an antenna, one quasi-elliptical mirror and two toroidal mirrors as beam-forming mirror system. Calculations show that the dimpled-wall launcher generates a well-focused TEM_{00} radiation pattern with low diffraction losses. Further calculations of power conservation show that an efficiency of more than 98% has been achieved to convert the rotating cavity $TE_{28,8}$ mode into a fundamental Gaussian beam. Low power measurements of the launcher and the beam-forming mirror system show that the beam patterns agree well with theoretical predictions.

Introduction

Current high power gyrotrons for nuclear fusion plasma applications employ an internal quasi-optical (q.o.) mode converter to transform the rotating high-order cavity mode into a linearly polarized fundamental Gaussian beam [1]-[3]. Conversion efficiencies close to unity are required since trapped RF energy jeopardizes the stable operation regime and may lead to heating of the inner tube structure. For a 1 MW continuous wave (CW) gyrotron operated in the $TE_{28,8}$ mode at 140 GHz, which is designed for the ECRH system of stellarator W7-X, in order to achieve a usable fundamental Gaussian output beam with very low diffraction losses, a highly efficient q.o. mode converter system with several novel features has been designed and tested at FZK. The design principal of a q.o. mode converter can be found in [4]; the following sections give more details about how to optimise the configuration of waveguide wall perturbations in order to obtain a well-focused Gaussian-like radiation from the launcher; the comparisons between measurement results (both low and high power measurements) and theoretical predictions are also given in this paper.

Design of the Quasi-Optical Mode Converter

This section reports on the optimised design of a q.o. mode converter of the 1 MW, 140 GHz, CW prototype gyrotron, operating in the $TE_{28,8}$ cavity mode for the stellarator W7-X. This operating mode belongs to a class of cavity modes for 1MW gyrotrons ($TE_{22,6}$, $TE_{25,10}$ and $TE_{31,8}$) for which the ratio of caustic to cavity radius is approximately 0.5. In this case the azimuthal bounce angle is $\Delta\varphi = 2\theta \approx 120^0$ and a $\Delta m_2 = 3$ perturbation of the dimpled-wall launcher provides perfect azimuthal focusing (Figure 1). The set of TE modes required to generate a Gaussian-like field distribution is given in Table 1.

$TE_{26,9}$ (0.03)	$TE_{29,8}$ (0.11)	$TE_{32,7}$ (0.03)
$TE_{25,9}$ (0.11)	$TE_{28,8}$ (0.44)	$TE_{31,7}$ (0.11)
$TE_{24,9}$ (0.03)	$TE_{27,8}$ (0.11)	$TE_{30,7}$ (0.03)

Table 1. Set of TE-modes to generate a Gaussian-like field distribution (with relative power).

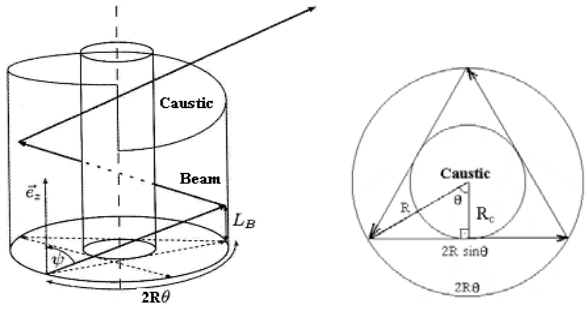

(a) (b)

Figure 1. Geometrical optical description of ray propagation in a cylindrical waveguide: (a) side view; (b) top view.

The current analysis method for these launcher systems is performed in two steps. First, the waveguide mode converter is analysed using coupled mode theory. Then, the radiated fields are calculated from the aperture field distribution at waveguide cut using the scalar diffraction integral. The launcher employs an irregular cylindrical waveguide section (pre-bunching section) followed by a helical-cut launching aperture, as shown in Figure 2. In the pre-bunching section prior to the launcher, a Gaussian profile of the field intensity on the waveguide wall can be achieved by specific periodic $\Delta m_1 = 1$ and $\Delta m_2 = 3$ wall deformations. There are two principal design criteria for the dimpled-wall waveguide section. First, the section must convert the main mode to a mixture of modes such that 100% of the power in the waveguide is contained in a bundle with a Gaussian-like amplitude profile. Second, this profile must be achieved within a short distance, typically less than 200 mm, so that the launcher is short enough to avoid interception of the expanding spent electron beam.

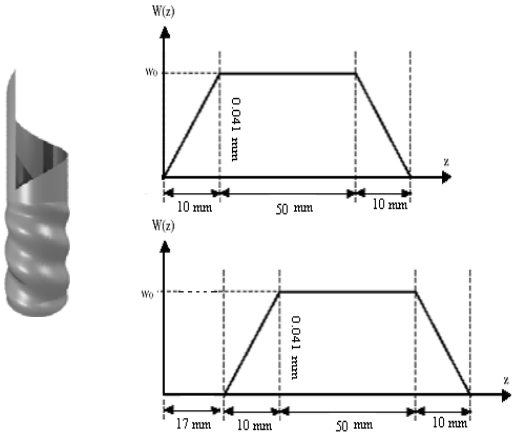

Figure 2. Schematic drawing of the dimpled-wall launcher and its wall deformations.

The design parameters for this launcher are: input radius of the waveguide section $a_0 \approx 21.9$ mm, the mean radius of the launcher section is slightly up-tapered ($R = a_0 + 0.004\,z$). This configuration reduces the Q factor of the section between the cavity and the helical cut, and suppresses spurious oscillations generated by the spent electron beam of the gyrotron in the launcher section. As shown in Figure 2, the $\Delta m_1 = 1$ and $\Delta m_2 = 3$ wall perturbations for longitudinal and azimuthal field bunching, respectively, use the same amplitude of 0.041 mm and perturbation length of 70 mm (with 10 mm tapers), but they start at different positions along the z-axis of the launcher. The $\Delta m_1 = 1$ perturbation is between z = 0 mm and z = 70 mm; the $\Delta m_2 = 3$ is between z = 17 mm and z = 87 mm. The helical cut of the antenna is located at 5.027 rad and begins at z = 159.7 mm. The cut length is 54.7 mm, the Brillouin angle 1.130 rad, and the azimuthal spread angle $\theta = 1.086$ rad.

Figures 3 and 4 show analysis results of the coupled mode calculations of the helical mode converter for the $TE_{28,\,8}$ mode at 140 GHz. In Figure 3, the variation of the mode composition along the length of the converter is plotted. At z = 0, corresponding to the start of the wall variation, a pure rotating $TE_{28,8}$ mode is injected. As the radiation travels along the z-axis, power in the $TE_{28,\,8}$ mode is coupled into mainly eight satellite modes through the wall perturbations. There are strong couplings from the $TE_{28,8}$ mode to the four satellite modes $TE_{27,8}$, $TE_{29,8}$, $TE_{25,9}$ and $TE_{31,7}$. Because of symmetry, with same perturbation two satellite modes obtain almost the same coupled power from the $TE_{28,8}$ mode.

Other additional modes that couple to the $TE_{28,8}$ mode through the waveguide wall deformations are also included in the analysis, since these modes serve to increase the peak amplitude of the Gaussian field distribution and decrease the levels of sidelobes of power. Figure 4 shows the calculated contour map of the

electrical field on the unrolled waveguide wall of the launcher. The shaped beam has weak fields (low diffraction losses) at the cut edge (indicated by the lines in Figure 4) and a nearly Gaussian angular spectrum. The Gaussian output pattern requires a certain amplitude and phase relation between the main mode and the satellite modes. The appropriate amplitude relation can be achieved with a short perturbed section of 70 mm. A longer smooth section follows and allows for the development of the optimum phase relations [5]. With this technique a shorter launcher can be built in comparison to a perturbed section that covers the whole length of the launcher [6].

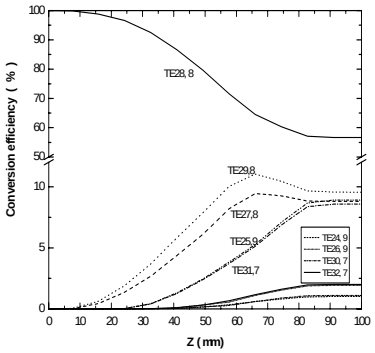

Figure 3. Mode composition (relative power) coefficients vary along the z-axis.

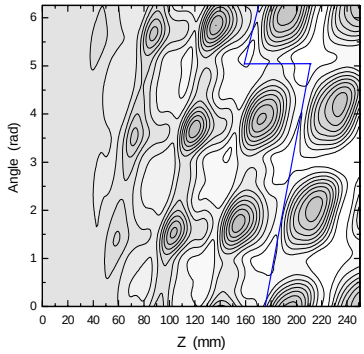

Figure 4. Contour map of the electrical field of a dimpled-wall launcher on its unrolled waveguide wall.

.

The radiation is launched from the prebunching section by cutting the waveguide wall around one Gaussian bundle, where the wall currents are at a minimum. The scalar diffraction integral was used to simulate the radiation of the aperture fields and to examine the properties of the launched beam. With the scalar diffraction integral, the fields at an observation point are calculated by integrating the response to the point source Green's function over all source regions. Due to the low fields along the edges of the straight and helical cuts, this advanced dimpled-wall launcher generates a well-focused Gaussian-like radiation pattern with low diffraction losses. In this case, combined with a quasi-elliptical mirror, two toroidal mirrors can be used as the beam-forming mirror system to obtain a desired beam pattern on the gyrotron output window, since calculations also show that smooth toroidal mirrors are sufficient; at the same time, they are inexpensive, easy to manufacture, and relatively easy to align.

With this beam-forming mirror system, further calculation of the power conservation from the launching waveguide shows that an efficiency of more than 98% has been achieved to convert the high-order cavity $TE_{28,8}$ mode at the frequency of 140 GHz into the fundamental Gaussian beam.

Experimental Measurements and Comparisons

A low power test facility has been built to check the performance of the q.o. mode converter system. The transmission measurement device consists of a vector network analyzer (VNWA), a low power $TE_{28,8}$ mode generator, the mode converter-system as device under test, and a pick-up antenna to measure the E-field distribution in a defined linear polarization (horizontal or vertical). The set-up and performance of the VNWA has been discussed in [7]. The pick-up antenna is fixed on a programmable 3-dimensional movable table in order to scan the distribution at an arbitrary position. High power measurements were performed with a dielectric target plate and an IR video camera.

A new q.o. $TE_{28,8}$ mode generator for low power test has been designed and fabricated. After accurate alignment of the mode generator, a high purity excitation of the desired mode has been possible. Measurements show that the counter-rotating mode has less than 0.3% of the total power.

To compare with theoretical predictions, cold measurements have been done in two steps: 1. The radiated field distribution from the launcher aperture on a plane at the distance of x = 100 mm from the launcher axis. 2. Power density distribution of the output beam at different distances from the gyrotron window. Figure 5 shows the comparison of cold measurement and calculation of the radiated electrical field distribution from the launcher aperture. They are in very reasonable agreement. After exact adjustment of the beam-shaping mirror system, further low power measurements of the gyrotron output beam at different positions have been done, as shown in Figure 6 (middle column). If one compares with theoretical predictions, which are also shown in Figure 6 (upper column), it is obvious that cold measurements and calculations give the identical output beam patterns in both near field and far field. They agree well with each other at different positions outside the gyrotron output window. A mode analysis reveals more than 96% fundamental Gaussian content.

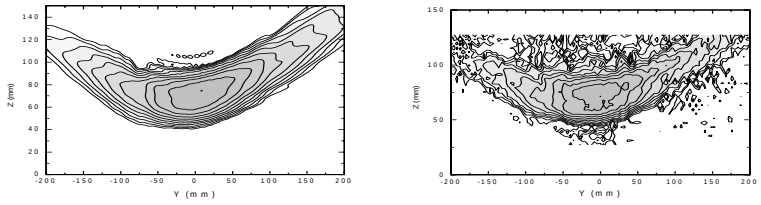

(a) (b)

Figure 5. Radiated field distribution on a plane at the position of 100 mm from the launcher axis. (a) Calculation; (b) Cold measurement.

Figure 6 (lower column) also shows high power measurement results viewed by an IR camera on a dielectric plate at three different distances from the gyrotron window. These hot measurements also show very reasonable agreement with both cold measurements and calculations. Probably due to minor

mechanical tolerances of the built-in gyrotron mode converter, the hot test show a somewhat more astigmatic Gaussian beam. Nevertheless, high power calorimetric measurements after a series of 2 mirrors and a circular polarizer reveal the very high directed beam content of approximately 97%.

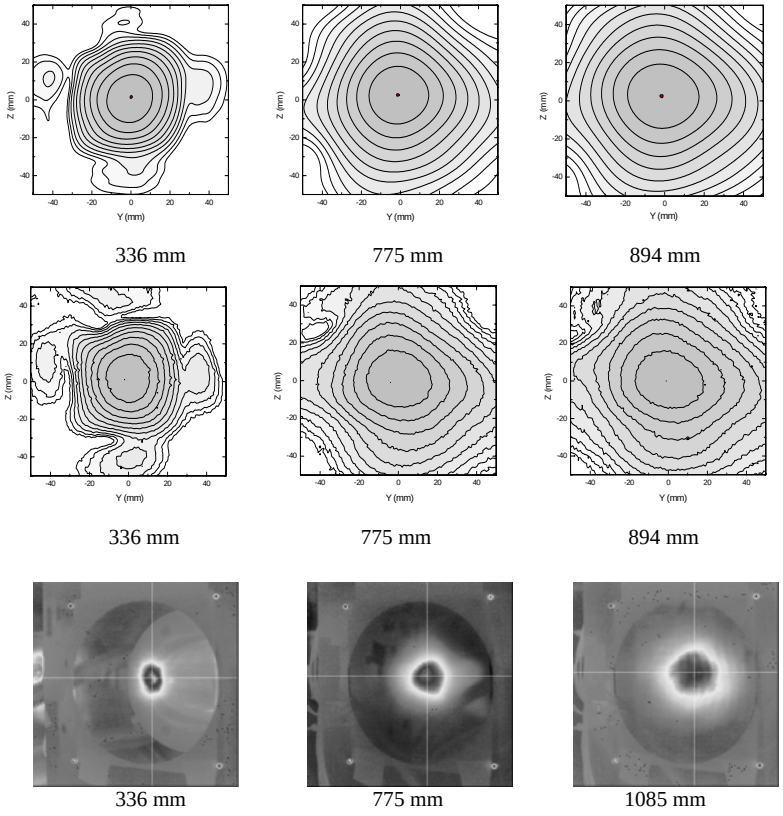

Figure 6. Comparisons of calculations (upper column), low power measurements (middle column) and high power measurements (lower column) at three different distances from the window.

References

[1] G. G. Denisov, et al., *Int. J. Electron*., vol.72, pp.1079-1091, 1992.

[2] J. Pretterebner, et al., in *Conf. Dig. 17th Int. Conf. on Infrared and Millimeter Waves*, Pasadena, CA, 1992, SPIE 1929, pp.40-41.

[3] M. Thumm, et al., *Fusion Eng. Des*., vol.53, pp.407-421, 2001.

[4] M. Thumm and W. Kasparek., *IEEE Trans. Plasma Sci.*, vol. 30, pp.755-786, 2002.

[5] J. Pretterebner, Ph.D Thesis, IPF, University Stuttgart, 2003.

[6] X. Yang, et al., *Int. J. Infrared Millimeter Waves*, vol. 24, pp. 1599-1608, 2003.

[7] O. Braz, et al., *in Proc. 22nd Int. Conf. on Infrared and Millimeter Waves*, Wintergreen, Virginia, USA, 1997, pp. 21-22.